Flow Loop Study of ECT-Based Volume Fraction Monitoring in Oil-Water Two-Phase Flows

Rafiul K. Rasel, Benjamin Straiton, Qussai Marashdeh, *Senior Member, IEEE*, and Fernando Teixeira, *Fellow, IEEE*

***Abstract*—Measurement of phase volume fractions in water-containing multiphase flows is necessary for the optimization of a host of industrial flow processes. Many water-containing multiphase flows can be classified as either water-dispersed or water-continuous mixtures. A recently developed approach based on Hanai's mixture formula and utilizing electrical capacitance tomography (ECT) sensors have shown good potential for obtaining water volume fraction estimates in two-phase water-containing flows with different water salinity levels. However, the proposed approach was investigated via controlled experiments restricted to static configurations while, in practice, multiphase flows can be dynamic and unpredictable. In this work, we perform a flow loop study of the proposed ECT-based method for volume fraction estimation in oil-water two-phase flows. We evaluate the performance of the proposed method in both water-dispersed and water-continuous flow regimes by employing different types of capacitive sensors in cylindrical arrangements and in parallel-plate rectangular arrangements.**

***Index Terms*—Electrical capacitance tomography, two-phase flows, water-cut, capacitive sensors, cross-plane measurements, process tomography, real time sensing.**

I. Introduction

MEASUREMENT of water volume fraction in multiphase flows is a common and challenging problem encountered across a wide range of industrial processes [1]–[4]. The ratio of the water volume compared to the total volume of liquid in the flow is often dubbed the "water cut". Several potential sensor modalities are available to monitor multiphase flows such as electrical capacitance tomography (ECT), displacement-current phase tomography (DCPT), electrical impedance tomography (EIT), X-Ray, MRI, and optical probes. Although accurate, X-Rays and MRI are expensive and optical probes are intrusive to the flow and may not be suitable in many industrial flow settings [5], [6]. ECT is a low-cost and non-intrusive alternative suitable for deployment in harsh industrial environments [7]–[18]. However, volume fraction determination in multiphase flows is a challenging problem for ECT especially when high water volume fractions are present. The difficulties arise mainly due to the high conductivity and permittivity of water [19]–[25]. In addition, the permittivity and conductivity of water depend on the salinity level [26], [27]. For two-phase flows, this challenge is somewhat mitigated by the fact that the constitutive properties of a two-phase mixture at sufficiently low frequencies depend primarily on the volume fraction and constitutive properties of the continuous phase [28]–[33].

In a previous work, we considered an approach using Hanai's mixture formula and ECT sensors to estimate the volume fraction in both water-dispersed and water-continuous two-phase flows [34]. The proposed approach was evaluated using simulations and preliminary controlled experiments involving static configurations. However, real-life monitoring of multiphase flows requires consideration of dynamic flows. Recently, a flow loop study of a deep learning-based water dispersed/continuous classifier for water-containing flows was carried out in [35]. The preliminary study in [35] was focused on the *classification* problem only and restricted to traditional ECT sensor configurations. In the present work, we evaluate the method considered in [34] for the *quantitative* monitoring of water volume fraction *levels* in two-phase flows using flow loop controlled experiments with two different types of capacitive sensors, viz. a traditional cylindrical ECT sensor, and a parallel-plate rectangular capacitance sensor. The present study provides further insight into the capabilities of the proposed method for the measurement and monitoring of water cuts in two-phase industrial flows.

II. Method of Analysis

Hanai's formula for complex dielectric, an extension of the Bruggeman formula, can provide an accurate estimation of the *complex* permittivity of homogeneously dispersed mixtures with possibly conducting phases [36], [37]. Hanai's formula for the complex dielectric of a mixture is given implicitly as:

$$\left(\frac{\epsilon_d^* - \epsilon_c^*}{\epsilon_d^* - \epsilon_m^*}\right)^3 \frac{\epsilon_m^*}{\epsilon_c^*} = \frac{1}{(1-\varphi_d)^3} = \frac{1}{\varphi_c^3}, \tag{1}$$

where ϵ_d^*, ϵ_c^*, and ϵ_m^* are the complex permittivities of the dispersed phase, the continuous phase, and the mixture, respectively. Moreover, φ_d is the volume fraction of dispersed phase and $\varphi_c = 1 - \varphi_d$ is volume fraction of the continuous phase. When $\epsilon_d^* \gg \epsilon_c^*$, Eq. (1) is valid for $0 \leq \varphi_d \lesssim 0.4$; and when $\epsilon_d^* \ll \epsilon_c^*$, Eq. (1) is valid for $0 \leq \varphi_d \lesssim 0.6$ [28]. If we denote the (angular) frequency of operation as ω, the free-space permittivity as ϵ_0, the (real) permittivities of the dispersed phase, continuous phase, and mixture as ϵ_d, ϵ_c, and ϵ_m, respectively (and similarly for the conductivities σ_d, σ_c and σ_m), then the complex permittivities in Eq. (1) can be

This work was supported in part by the U. S. Department of Energy cooperative agreement DE-FE0031858.

R. K. Rasel and F. Teixeira are with the ElectroScience Laboratory, Department of Electrical and Computer Engineering, The Ohio State University, Columbus, OH 43212 USA (e-mail: rasel.1@osu.edu, teixeira.5@osu.edu).

B. Straiton and Q. Marashdeh are with Tech4Imaging LLC, Columbus, OH 43220 USA (e-mail: ben@tech4imaging.com, marashdeh@tech4imaging.com).

R. K. Rasel, B. J. Straiton, Q. M. Marashdeh, and F. L. Teixeira, "Flow Loop Study of ECT-Based Volume Fraction Monitoring in Oil–Water Two-Phase Flows," IEEE Trans. Instrum. Meas., vol. 71, pp. 1–6, 2022, doi: 10.1109/TIM.2022.3181929.
https://doi.org/10.1109/TIM.2022.3181929

written as $\epsilon_d^* = \epsilon_d - j\sigma_d/\omega\epsilon_0$, and likewise for ϵ_c^* in terms of ϵ_c and σ_c, and for ϵ_m^* in terms of ϵ_m and σ_m.

At sufficient low frequencies, when $\sigma_c \neq 0$ and $\epsilon_c \ll \sigma_c/\omega\epsilon_0$ and/or $\epsilon_d \ll \sigma_d/\omega\epsilon_0$, i.e. the effect of conductivity is predominant. Consequently, Hanai's formula can be approximated in terms of the conductivities as [28]

$$\left(\frac{\sigma_d - \sigma_c}{\sigma_d - \sigma_m}\right)^3 \frac{\sigma_m}{\sigma_c} \approx \frac{1}{(1-\varphi_d)^3} = \frac{1}{\varphi_c^3}. \tag{2}$$

A. Low Frequency Estimates for $\sigma_c \approx 0$ and $\sigma_d \neq 0$

If the conductivity of the continuous phase is negligibly small ($\sigma_c \approx 0$), Hanai's formula for complex dielectric constant of the mixture,

for water-dispersed flow ($\epsilon_d \gg \epsilon_c, \epsilon_m$), reduces to [28], [34]

$$\frac{\epsilon_m^*}{\epsilon_c^*} \approx \frac{1}{(1-\varphi_d)^3}. \tag{3}$$

A low-frequency estimation of φ_d from these relations leads to $\varphi_d \approx 1 - (\epsilon_c/\epsilon_m)^{1/3}$, and $\varphi_d \approx 1 - (\sigma_c/\sigma_m)^{1/3}$. which means that, at sufficiently low frequencies, the volume fraction of each phase in a multiphase flow can be estimated from the permittivity and conductivity values of the continuous phase and the mixture alone. Since σ_m and σ_c can be negligibly small for this flow type, the permittivity formulation is expected to provide better estimates.

B. Low-Frequency Estimates for $\sigma_c \neq 0$ and $\sigma_d \approx 0$

If $\sigma_c \neq 0$ and $\sigma_d \approx 0$, Hanai's formula for the complex permittivity of the mixture, for water-continuous flow ($\epsilon_c, \epsilon_m \gg \epsilon_d$), can be rewritten as [28], [34]

$$\left(\frac{\epsilon_c^*}{\epsilon_m^*}\right)^2 \approx \frac{1}{\varphi_c^3}. \tag{4}$$

Therefore, the low-frequency limit of Eq. (1) yields $\varphi_c \approx (\epsilon_m/\epsilon_c)^{2/3}$ and $\varphi_c \approx (\sigma_m/\sigma_c)^{2/3}$. From these relations, it is clear that at sufficiently low frequencies, the volume fraction can be calculated from the permittivity and conductivity values of the continuous phase and the mixture. Further details about this method of approach are presented in [34].

C. Initial Data Calibration

The Hanai's formula based (HFB) volume fraction estimates for φ_d and φ_c obtained in the previous section do not account for the particular sensor setup and geometry such as the finite-sized electrode plates, the vessel thickness and radius, and additional factors such as electric field fringing effects. All these factors play a role in the measured capacitance values. Therefore, HFB theoretical estimates establish expected baseline dependencies among the volume fraction and flow parameters but for better results in practice, it is necessary to make room for the additional factors unaccounted for by the theoretical estimates [34]. For a given water-containing flow type (either water-continuous or water dispersed), the following general relation between the HFB estimates and the calibrated estimates was found to provide a good tradeoff between simplicity, generality, and accuracy:

$$\tilde{\varphi} = \left(\frac{\varphi}{\varphi_\phi}\right)^\alpha \phi, \tag{5}$$

where φ and $\tilde{\varphi}$ are the HFB estimate and the calibrated water volume fractions, respectively, and φ_ϕ is the HFB estimate volume fraction of water when the actual (known) volume of water fraction present in the flow is ϕ. The exponent α primarily depends on the geometry of the vessel, sensor design, and the flow type (i.e., either water-continuous or water-dispersed). For a given sensor and flow type, this parameter can be determined using data from a few initial calibration experiments.

These experimental calibration values can be stacked onto a (known) fractional water volume column vector denoted using an overbar as $\bar{\tilde{\phi}}$. Likewise, a corresponding HFB-estimated volume fraction column vector can be defined and denoted as $\bar{\varphi}$. To determine the value of α, Eq. (5) can be rewritten in terms of the known and HFB-estimated volume vector as $\bar{\tilde{\phi}} = (\bar{\varphi}/\varphi_\phi)^\alpha \phi$ and using a least square fit, the value of α is given by $\alpha = \bar{\tilde{\varphi}}_l^t \cdot \bar{\varphi}_l / \|\bar{\varphi}_l\|^2$, where $\cdot$ denotes inner product, $\bar{\tilde{\varphi}}_l = \ln(\bar{\tilde{\varphi}}/\phi)$, $\bar{\varphi}_l = \ln(\bar{\varphi}/\varphi_\phi)$, and the superscript t denotes transpose.

III. Results

Two-phase flow experiments were carried out in the flow loop shown in Fig. 1a. Two types of sensors were used: (a) A 9.5×9.5 cm parallel-plate capacitance sensor shown in Fig. 1b and (b) a conventional 4×2 ECT sensor shown in Fig. 1c. The height of each electrode of the ECT sensor is 9.5 cm, the gap between two electrodes along the azimuth is 9°, and the gap between electrodes in the vertical direction is about 1.25 cm. Multiple two-phase flow experiments with varying phase volume fractions were carried out using industrial grade white oil ($\epsilon_o \approx 2.5,\ \sigma_o \approx 0\ mS/m$) and tap water ($\epsilon_w \approx 81,\ \sigma_w \approx 5\ mS/m$).

Fig. 2 shows a schematic diagram of the flow loop used in the experiment. The flow loop includes a reservoir to store oil and water, a water pump, and an oil pump to deliver specific volumes of water and oil into the system. There is a Coriolis meter right after the water and oil pump to accurately measure the water-cut delivered into the system. The flow loop uses stainless steel pipes throughout the loop except for the capacitive sensing region, where a PVC pipe is used to enable the electric fields from the ECT sensor to penetrate into the flow region. The inner and outer vessel diameters of the PVC pipe in the ECT sensing region are 6.35 cm and 4.7 cm, respectively. This particular method is specifically suitable for spherically dispersed homogeneous flows and may work for other homogeneously dispersed flow regimes. Therefore, to ensure the homogeneity of the flow, a mixer is placed right before the ECT sensor.

The typical salinity of freshwater lies below 1 ppt (parts per thousand) and can vary depending on several factors. For water-dispersed flows, higher salinity should not impact the results as long as the measurement frequency is sufficiently

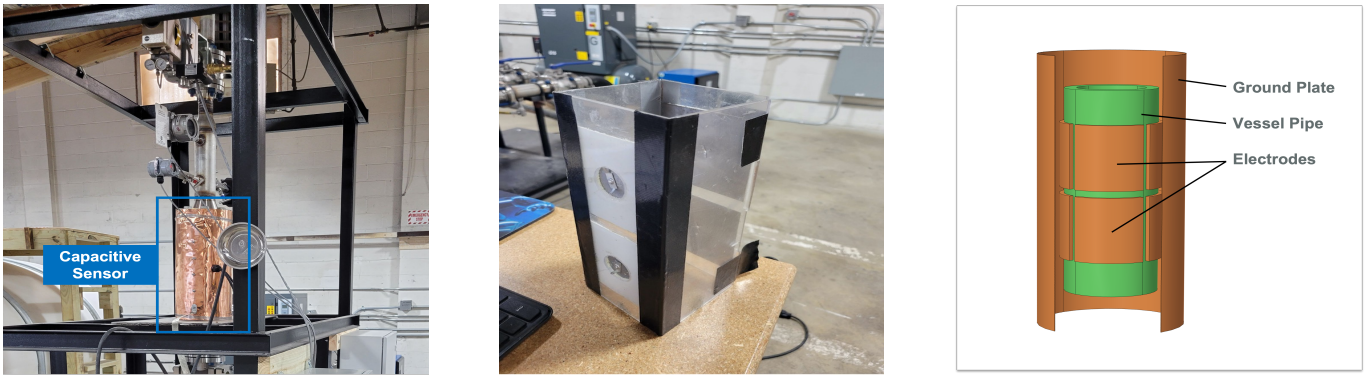

Fig. 1. (a) Image of the flow loop where the sensor is mounted. (b) image of the parallel-plate capacitance sensor used in the experiment, and (c) 3-D model of the ECT sensor used in the experiment.

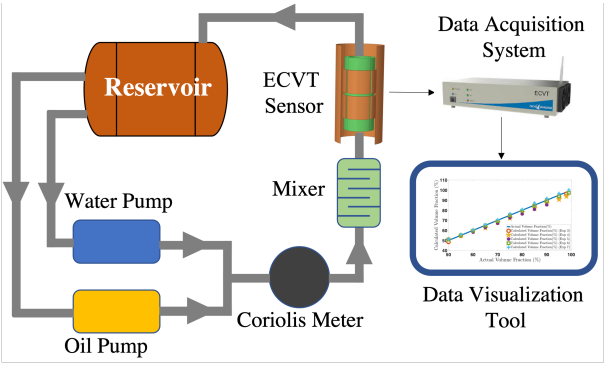

Fig. 2. Diagram of the flow loop, consisting of a reservoir, a water-pump, an oil pump, a Coriolis meter, a mixer, and a capacitive (ECT) sensor, respectively.

low for the low-frequency estimation method described in Section II to apply. For water-continuous flows, higher salinity may introduce some measurement difficulties due to the high conductivity and skin effect. Therefore, it is important to have an estimate of the water salinity so that the measurement can be obtained at proper frequencies. To evaluate the proposed technique, a total of eight rounds of experiments were conducted using the flow loop, denoted as Exp 1-8 in what follows. Each round included both water-dispersed and water-continuous flows. Two experimental rounds involved the parallel plate capacitance sensor and the remaining five the conventional ECT sensor.

Measurements were obtained with a frame rate of 761 fps (frame-per-second) for the parallel plate sensor and 361 fps for the ECT sensor. Admittance measurements were obtained by exciting electrodes with a 2 MHz input voltage signal and measuring the current at the terminal of the remaining electrodes. From the results, it is clear that the measurement obtained at 2 MHz is sufficient for low-frequency volume estimation at the water salinity levels considered in the experiments. However, depending on the salinity levels, 2 MHz measurement may not be low enough for volume estimation. The real and imaginary parts of the admittance data can be associated with the conductivity and permittivity of the flow, respectively. A total of 20,000 to 60,000 frames per measurement were collected. We found that the multiphase flow stabilizes after approximately 5-10 minutes (10,000-20,000 frames) and measurements from the stabilized region were used for comparison with ground truth values. The typical signal-to-noise ratio (SNR) of the instruments used in the experiment is around 60 dB [31].

A. *Water-Dispersed Flow*

Water is dispersed in oil for two-phase water-dispersed flows. The presented method utilizes real components of the measured data (e.g., *permittivity*) to calculate water volume from the water-dispersed flows.

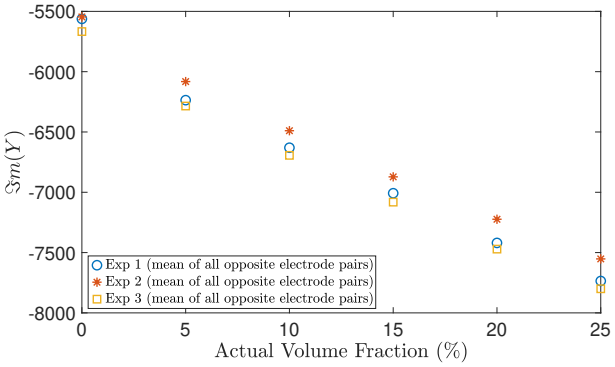

Fig. 3. Imaginary part of the raw admittance data Y, obtained by taking the mean of all opposite electrode pairs. Data are presented for water-dispersed experiments.

TABLE I
ESTIMATED WATER VOLUME IN TWO-PHASE WATER-DISPERSED FLOWS: PARALLEL-PLATE SENSOR RESULTS

	0%	5%	10%	15%	20%	25%
Exp 1	0.4	5.1	9.6	**15**	21.5	27
Exp 2	0.3	3.6	7.9	13	18.4	23.8
Exp 3	0.61	4.7	9.1	14.3	20.2	25.8

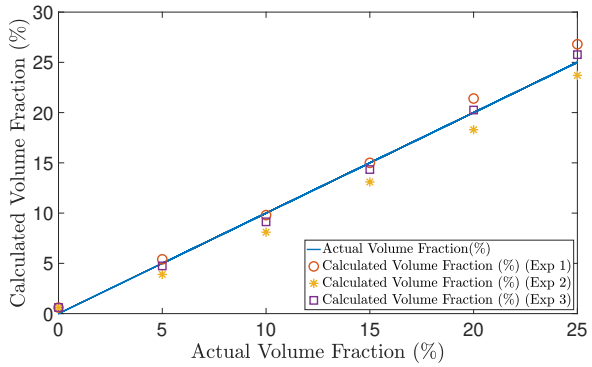

Fig. 4. Estimated water volume fraction obtained from two-phase water-dispersed flows using parallel-plate sensor. Results are presented for two different experimental rounds.

1) Parallel-Plate Capacitance Sensor: Fig. 4 and Table I show the calculated volume fraction of water obtained from two-phase water-dispersed multiphase flows using the parallel plate sensor. Results are presented for two experimental rounds using the parallel plate sensor i.e., Exp 1, 2, and 3. For the results in Fig. 4 and Table I, 15% water volume data from Exp 1 was used to obtain the calibration factors φ_ϕ and ϕ. The value of $\alpha = 2$ provided the best results for this sensor and flow type. Since the initial calibration uses data from Exp 1, the results for that dataset provide a better estimation compared to the results presented for the Exp 2 dataset. An average absolute error of less than 2% indicates that the estimated volumes are in good agreement with the actual volumes, denoted by a blue line in the figures. The minor discrepancy in the estimated volumes between Exp 1 and Exp 2 may be attributable to the discrepancy in the measured data shown in Fig. 3.

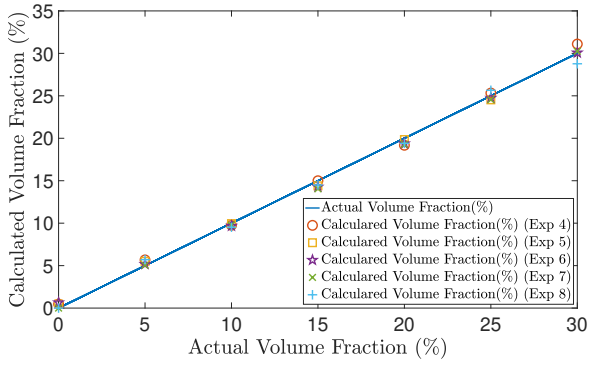

Fig. 5. Calculated water volume fraction obtained from two-phase water-dispersed flows using the conventional ECT sensor. Results are presented for five different experimental rounds.

2) Conventional ECT Sensor: Fig. 5 and Table II show the calculated water volume fraction obtained using a conventional ECT sensor for two-phase water-dispersed flows. The five experimental rounds, in this case, are denoted as Exp 4, 5, 6, 7, and 8. Although in principle any (set of) electrode pairs could be used for the mutual admittance measurements, in our study we found that it is best to avoid

TABLE II
ESTIMATED WATER VOLUME IN TWO-PHASE WATER-DISPERSED FLOWS: ECT SENSOR RESULTS

	0%	5%	10%	15%	20%	25%	30%
Exp 4	0.5	5.7	9.8	**15**	19.2	25.3	31.1
Exp 5	0.5	5.5	10	14.4	19.9	24.5	n/a
Exp 6	0.6	5.2	9.7	14.3	19.4	24.8	30.1
Exp 7	0.1	5.1	9.8	14.1	19.3	24.6	30.3
Exp 8	0.0	5.2	9.5	14.5	19.5	25.7	28.8

adjacent electrode pairs, especially when the flow is water-continuous. We conjecture that this might be due to local electric field fringing effects. Therefore, the results are based on mutual admittance measurement between opposite electrodes in the ECT sensor. The calibration factors are calculated based on the 15% water volume data from Exp 4. In this case, $\alpha = 1.5$ was found to provide better estimates. The calculation error in the presented results is approximately 1%. Note that n/a denotes that the data was either poor or unavailable.

B. Water Continuous Flow

For two-phase water-continuous flows, oil is dispersed in water. In order to calculate the water volume fraction in water-continuous flows, only the real part of the measured admittance (associated with the conductivity) is used.

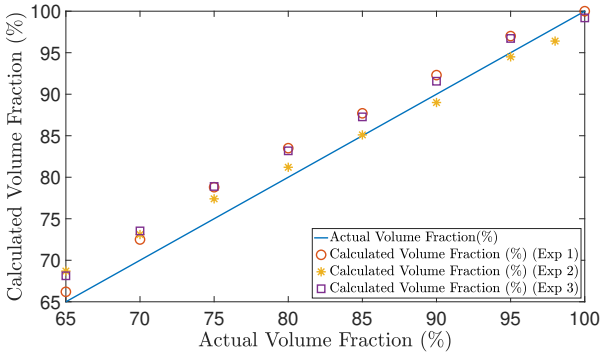

Fig. 6. Estimated water volume fraction obtained from two-phase water-continuous flows using the parallel-plate sensor. Results are presented for two rounds of experiments.

TABLE III
ESTIMATED WATER VOLUME IN TWO-PHASE WATER-CONTINUOUS FLOWS: PARALLEL-PLATE SENSOR RESULTS

	65%	70%	75%	80%	85%	90%	95%	100%
Exp 1	66.2	72.5	78.8	83.5	87.7	92.3	97	**100**
Exp 2	68.7	73.1	77.4	81.2	85.1	89	94.5	n/a
Exp 3	68.13	73.5	78.8	83.1	87.2	91.5	94.5	99.2

1) Parallel-Plate Capacitance Sensor: Fig. 6 and Table III show the calculated water volume obtained for the two-phase water dispersed flow using the parallel plate sensor. Results are presented for Exp 1, 2, and 3. The calibration factor was calculated based on the 100% water volume data from Exp 1. The value of $\alpha = 1$ provides a more accurate estimation for

this sensor setup and flow type. The calculated results are in good agreement with the actual data (blue line in the figure), with an average error below 3%.

2) Conventional ECT Sensor: Fig. 7 and Table IV show the calculated water volume obtained from two-phase water-continuous flows using the conventional ECT sensor. Results are presented for Exp 4, 5, 6, 7, and 8. Measurements from opposite electrode pairs were used to estimate the water volume. The calibration step used the 75% water volume data from Exp 7. For this sensor configuration and flow type $\alpha = 1.2$ provides the best estimates. The average absolute error in the estimated is about 2%. However, from the results presented for the parallel plate sensor and the ECT sensor, it is apparent that the ECT sensor provides slightly better volume fraction estimates. This could be attributed to the shape of the ECT sensor, which better conforms to the shape of the flow-carrying vessel.

In our study, we found that the flow regime classification into either water dispersed or water continuous becomes ambiguous when the water volume fraction is between about 30%−50%. In this range, the flow regime gradually changes from water-dispersed to water-continuous, and a clear-cut classification is not possible. As a result, the presented method was not able to provide accurate volume estimates in this volume range.

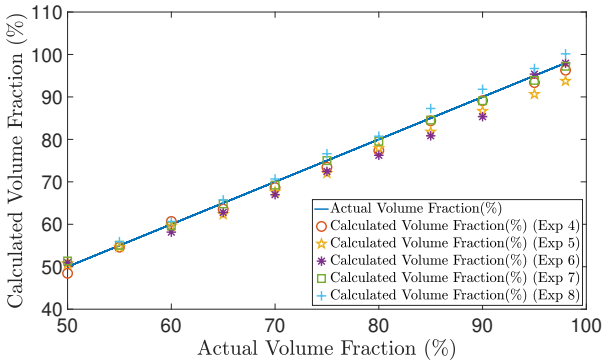

Fig. 7. Estimated water volume fraction obtained from two-phase water-continuous flows using the conventional ECT sensor. Results are presented for five different experimental rounds.

TABLE IV
ESTIMATED WATER VOLUME IN TWO-PHASE WATER-CONTINUOUS FLOWS: ECT SENSOR RESULTS

	50%	55%	60%	65%	70%	75%	80%	85%	90%	95%	99%
Exp 4	48.5	54.6	n/a	63.6	68.7	73.5	77.4	84.4	89.1	93.4	96.3
Exp 5	50.8	54.6	59.6	62.3	67.6	72.0	77.9	81.8	86.7	90.6	93.8
Exp 6	50.7	n/a	58.2	62.8	67.0	72.5	76.3	80.9	85.4	95.6	98.2
Exp 7	51.0	55.1	59.7	64.8	69.2	**75**	79.6	84.6	89.1	93.9	97.2
Exp 8	51.4	55.9	60.7	65.8	70.7	76.6	80.8	87.3	91.8	96.7	100.1

IV. Conclusions and Future Work

In this paper, we performed a flow loop study of the method outlined in [34] for estimating water volume fraction in two-phase flows. In most of the considered cases, the average absolute error in the volume fraction results was below 3%. The method is mostly applicable for homogenized flows with fractional water volume ranges unambiguously characterized as either water dispersed or water continuous. The sensing domain consisted of a vessel with a cylindrical cross-section; however, the results show the robustness of the method regardless of whether a cylindrical sensor or a parallel plate sensor is used to measure the mutual admittance data. Although the presented method was able to accurately calculate water volume in two-phase flows under such conditions, the method requires a priori knowledge of the constitutive properties of the continuous phase for best results. In addition, for a given vessel and sensor configuration geometry, an initial calibration step is required based on known volume fraction levels. Work is currently underway to alleviate these requirements.

V. Acknowledgement

We thank Aron Reman for conducting the experiments at Tech4Imaging.

References

[1] L.-S. Fan, *Gas-Liquid-Solid Fluidization Engineering*. Boston: Butterworth-Heinemann, 1989.
[2] C. D. Han, "Multiphase flow in polymer processing," in *Rheology*. Springer, 1980, pp. 121–128.
[3] C. T. Crowe, *Multiphase flow handbook*. CRC press, 2005, vol. 59.
[4] L. M. Al-Hadhrami, S. Shaahid, L. O. Tunde, and A. Al-Sarkhi, "Experimental study on the flow regimes and pressure gradients of air-oil-water three-phase flow in horizontal pipes," *The Scientific World Journal*, vol. 2014, 2014.
[5] J. Xue, M. Al-Dahhan, M. Dudukovic, and R. Mudde, "Four-point optical probe for measurement of bubble dynamics: Validation of the technique," *Flow Measurement and Instrumentation*, vol. 19, no. 5, pp. 293–300, 2008.
[6] F. Hamad, F. Imberton, and H. Bruun, "An optical probe for measurements in liquid-liquid two-phase flow," *Measurement science and technology*, vol. 8, no. 10, p. 1122, 1997.
[7] S. Huang, C. Xie, J. Salkeld, A. Plaskowski, R. Thorn, R. Williams, A. Hunt, and M. Beck, "Process tomography for identification, design and measurement in industrial systems," *Powder Technology*, vol. 69, no. 1, pp. 85 – 92, 1992.
[8] D. Watzenig and C. Fox, "A review of statistical modelling and inference for electrical capacitance tomography," *Measurement Science and Technology*, vol. 20, no. 5, p. 052002, 2009.
[9] R. A. Williams and M. S. Beck, *Process Tomography*. Oxford: Butterworth-Heinemann, 1995.
[10] Q. Marashdeh and F. L. Teixeira, "Sensitivity matrix calculation for fast 3-D electrical capacitance tomography (ECT) of flow systems," *IEEE Transactions on Magnetics*, vol. 40, no. 2, pp. 1204–1207, March 2004.
[11] A. Wang, Q. Marashdeh, B. J. Motil, and L.-S. Fan, "Electrical capacitance volume tomography for imaging of pulsating flows in a trickle bed," *Chemical Engineering Science*, vol. 119, pp. 77 – 87, 2014.
[12] W. Warsito, Q. Marashdeh, and L. S. Fan, "Electrical capacitance volume tomography," *IEEE Sensors Journal*, vol. 7, no. 4, pp. 525–535, April 2007.
[13] K. J. Alme and S. Mylvaganam, "Electrical capacitance tomography–sensor models, design, simulations, and experimental verification," *IEEE Sensors Journal*, vol. 6, no. 5, pp. 1256–1266, Oct. 2006.
[14] S. Chowdhury, Q. M. Marashdeh, and F. L. Teixeira, "Velocity profiling of multiphase flows using capacitive sensor sensitivity gradient," *IEEE Sensors Journal*, vol. 16, no. 23, pp. 8365–8373, 2016.
[15] Q. M. Marashdeh, F. L. Teixeira, and L.-S. Fan, "Adaptive electrical capacitance volume tomography," *IEEE Sensors Journal*, vol. 14, no. 4, pp. 1253–1259, 2014.
[16] Y. S. Kim, S. H. Lee, U. Z. Ijaz, K. Y. Kim, and B. Y. Choi, "Sensitivity map generation in electrical capacitance tomography using mixed normalization models," *Measurement Science and Technology*, vol. 18, no. 7, p. 2092, 2007.
[17] Y. Li and D. J. Holland, "Fast and robust 3D electrical capacitance tomography," *Measurement Science and Technology*, vol. 24, no. 10, p. 105406, 2013.

[18] S. Chowdhury, Q. M. Marashdeh, and F. L. Teixeira, "Inverse normalization method for cross-sectional imaging and velocimetry of two-phase flows based on electrical capacitance tomography," *IEEE Sensors Letters*, vol. 2, no. 1, pp. 1–4, March 2018.
[19] Q. Marashdeh, W. Warsito, L. S. Fan, and F. L. Teixeira, "A multimodal tomography system based on ECT sensors," *IEEE Sensors Journal*, vol. 7, no. 3, pp. 426–433, March 2007.
[20] Q. Marashdeh, W. Warsito, , L. S. Fan, and F. L. Teixeira, "Dual imaging modality of granular flow based on ECT sensors," *Granular Matter*, vol. 10, no. 2, pp. 75–80, Jan. 2008.
[21] N. M. Hasan and B. J. Azzopardi, "Imaging stratifying liquid–liquid flow by capacitance tomography," *Flow Measurement and Instrumentation*, vol. 18, no. 5, pp. 241 – 246, 2007.
[22] K. Perera, C. Pradeep, S. Mylvaganam, and R. W. Time, "Imaging of oil-water flow patterns by electrical capacitance tomography," *Flow Measurement and Instrumentation*, vol. 56, pp. 23 – 34, 2017.
[23] M. Zhang and M. Soleimani, "Simultaneous reconstruction of permittivity and conductivity using multi-frequency admittance measurement in electrical capacitance tomography," *Measurement Science and Technology*, vol. 27, no. 2, p. 025405, 2016.
[24] Y. Li, W. Yang, C. gang Xie, S. Huang, Z. Wu, D. Tsamakis, and C. Lenn, "Gas/oil/water flow measurement by electrical capacitance tomography," *Measurement Science and Technology*, vol. 24, no. 7, p. 074001, 2013.
[25] Z. Cui, Y. Chen, and H. Wang, "A dual-modality integrated sensor for electrical capacitance tomography and electromagnetic tomography," *IEEE Sensors Journal*, vol. 19, no. 21, pp. 10 016–10 026, 2019.
[26] J. B. Hasted, D. M. Ritson, and C. H. Collie, "Dielectric properties of aqueous ionic solutions. parts i and ii," *The Journal of Chemical Physics*, vol. 16, no. 1, pp. 1–21, 1948. [Online]. Available: https://doi.org/10.1063/1.1746645
[27] N. Gavish and K. Promislow, "Dependence of the dielectric constant of electrolyte solutions on ionic concentration: A microfield approach," *Phys. Rev. E*, vol. 94, p. 012611, Jul 2016. [Online]. Available: https://link.aps.org/doi/10.1103/PhysRevE.94.012611
[28] P. Becher, *Dielectric Properties of Emulsions and Related Systems," Encyclopedia of Emulsion Technology*. New York: M. Dekker, 1983.
[29] J. C. Maxwell, *A Treatise on Electricity and Magnetism*. Clarendon: Oxford, 1892.
[30] K. W. Wagner, "The after effect in dielectrics," *Arch. Electrotech*, vol. 2, p. 378, 1914.
[31] R. K. Rasel, C. Zuccarelli, Q. Marashdeh, L. S. Fan, and F. L. Teixeira, "Towards multiphase flow decomposition based on electrical capacitance tomography sensors," *IEEE Sensors Journal*, vol. 17, no. 24, pp. 8027–8036, 2017.
[32] R. K. Rasel, C. Gunes, Q. M. Marashdeh, and F. L. Teixeira, "Exploiting the Maxwell-Wagner-Sillars effect for displacement-current phase tomography of two-phase flows," *IEEE Sensors Journal*, vol. 17, no. 22, pp. 7317–7324, 2017.
[33] R. K. Rasel, Q. Marashdeh, and F. L. Teixeira, "Toward electrical capacitance tomography of water-dominated multiphase vertical flows," *IEEE Sensors Journal*, vol. 18, no. 24, pp. 10 041–10 048, 2018.
[34] R. K. Rasel, B. Straiton, Q. Marashdeh, and F. L. Teixeira, "Toward water volume fraction calculation in multiphase flows using electrical capacitance tomography sensors," *IEEE Sensors Journal*, 2020.
[35] R. K. Rasel, B. J. Straiton, A. Solon, Q. M. Marashdeh, and F. L. Teixeira, "Deep learning based volume fraction estimation for two-phase water-containing flows," in *2021 IEEE Sensors*, 2021, pp. 1–4.
[36] T. Hanai, "Theory of the dielectric dispersion due to the interfacial polarization and its application to emulsions," *Kolloid-Zeitschrift*, vol. 171, no. 1, pp. 23–31, Jul 1960. [Online]. Available: https://doi.org/10.1007/BF01520320
[37] D. A. G. Bruggeman, "Berechnung verschiedener physikalischer konstanten von heterogenen substanzen," *Annalen der Physik*, vol. 416, no. 7, pp. 636–664, 1935. [Online]. Available: http://dx.doi.org/10.1002/andp.19354160705

Rafiul K. Rasel received the B.S. degree in electrical engineering (minored in mathematics) and M.S. degree in electrical engineering from the State University of New York at New Paltz, New Paltz, NY, USA in 2013 and 2015, respectively. He received the Ph.D. degree in electrical engineering at The Ohio State University, Columbus, OH, USA in 2019. He is currently a post-doctoral scholar with the ElectroScience Lab at The Ohio State University, Columbus, OH, USA. His research interests include multiphase flow, capacitive sensing, process tomography, inverse problems, and computational electromagnetics.

Benjamin Straiton received the B.S. degree in Electrical and Computer Engineering from The Ohio State University, Columbus, Ohio, USA in 2016. He is currently a product development manager for Tech4Imaging, LLC, advancing electrical tomography systems for industrial multiphase flow applications. His research interests include electrical tomography and multiphase flow systems.

Qussai Marashdeh received the B.S. degree in electrical engineering from the University of Jordan, Amman, Jordan, in 2001, and both the M.S. and Ph.D. degrees in electrical engineering while affiliated with the Electroscience Laboratory, The Ohio State University, Columbus, in 2003 and 2006, respectively. He also received the M.S in chemical engineering and the M.B.A. from The Ohio State University in 2009 and 2012, respectively.

He is cofounder, President, and CEO of Tech4Imaging LLC, a startup company aimed at advancing capacitance tomography technology and its applications. His research interests include electrical tomography systems, electrostatics, optimization, multiphase flow, and inverse problems.

Fernando Teixeira received the Ph.D. degree in electrical engineering from the University of Illinois, Urbana- Champaign in 1999. He was a Postdoctoral Associate with the Massachusetts Institute of Technology during 1999-2000. Since 2000, he has been with The Ohio State University, where he is now a Professor with the Department of Electrical and Computer Engineering and affiliated with the ElectroScience Laboratory.

Dr. Teixeira is a recipient of the NSF CAREER Award, the triennial Booker Fellowship from the International Union of Radio Science, and the Outstanding Young Engineer Award from the IEEE Microwave Society (MTT-S). He served as an Associate Editor for the IEEE ANTENNAS AND WIRELESS PROPAGATION LETTERS from 2008 to 2014 and current serves as Associate Editor for *IET Microwaves, Antennas, and Propagation*. His current research interests include electromagnetic sensors, computational electromagnetics, and inverse problems.